Pramana – J. Phys. (2022) 96:136
https://doi.org/10.1007/s12043-022-02381-4

Anharmonicity-induced criticality of the ground-state properties of attractive Bose–Einstein condensate

PANKAJ KUMAR DEBNATH

Swami Vivekananda High School, Garshyamnagar II, P.O. Shyamnagar, North 24 Parganas 743 127, India
E-mail: pankaj_phys@yahoo.com

MS received 8 February 2021; revised 22 June 2021; accepted 7 March 2022

Abstract. We consider the attractive Bose–Einstein condensate (BEC) of Rb atoms, which is confined in a harmonic plus quartic trap $[V(r) = \frac{1}{2}m\omega^2 r^2 + \lambda r^4]$. We slowly tune the coefficient of quartic term (λ) to see how the metastable region (MSR) in the outer part of the trap is modified. The MSR is always bounded by a left intermediate barrier (IB) and a deep but narrow attractive well (NAW) appears on the left of this barrier. For $\lambda < 0$, the MSR is bounded by an additional right IB. A dramatic behaviour (compared with the attractive BEC in a harmonic trap) of interaction energy, kinetic energy, trap energy along with the total ground-state energy of the condensate is observed in this different metastability. For $\lambda \geq 0$, the outer wall of the MSR increases steeply as λ increases. Dynamical responses of the zero point energies of the condensate are explored also. Observations are interesting as we find a critical value of anharmonicity (λ_{cr}) to collapse the condensate. We slightly increase the strength of λ (close to λ_{cr}) and investigate the significant increase of the quantum tunnelling probability through the left IB into an inner core (NAW).

Keywords. Bose–Einstein condensation; anharmonic trap; potential harmonics; hyperspherical harmonics.

PACS Nos **03.75.Hh; 31.15.Ja; 03.65.Ge**

1. Introduction

The behaviour of confined, Bose–Einstein condensed atoms has been extensively studied both experimentally [1–5] as well as theoretically. The form of external confinement potential is very crucial in these studies. In most of the earlier theoretical studies performed on the cold gases of atoms, the trapping potential was harmonic. It is interesting, however, that the harmonic trapping is special in many respects. For this reason, different theoretical studies [6–22] have considered traps with other functional forms, in which the trapping potential grows more rapidly than quadratically at distances far away from the centre of the cloud. In refs [23–25], a tuned laser ray was directed along the axial direction in a combination of pure magnetic trap. The tuned laser adds a quartic component to the usual harmonic potential, resulting in a confinement of the form

$$V(r) = \frac{1}{2}m\omega^2 r^2 + \frac{k}{4}r^4,$$

where m is the mass of the atom.

Motivated by these facts, we consider here a trapping potential which is harmonic with a quartic distortion, viz. $V_{\mathrm{trap}}(r) = \frac{1}{2}m\omega^2 r^2 + \lambda r^4$. We slowly tune the anharmonic parameter λ from harmonic to anharmonic, to study zero-temperature ($T = 0$) energies of the attractive condensate in this confinement. We choose ^{85}Rb atoms with $a_{\mathrm{sc}} = -1.832 \times 10^{-4}$ o.u., which is one of the choices of scattering length a_{sc} in the controlled collapse experiment of Roberts *et al* [26–28]. We employ a method, called the potential harmonic (PH) expansion method, which is actually an extension of hyperspherical harmonic (HH) expansion method under certain approximations [29–31]. The PH is a subset of HH where all correlations higher than two-body ones are disregarded. This choice is justified since the experimental condensate is very dilute. A realistic interatomic interaction is incorporated in our method which is very essential for attractive BEC.

It is well known that although the attractive homogeneous Bose–Einstein condensate (BEC) is unstable, the external confinement makes it metastable if the number of atoms (A) is below a certain critical number (A_{cr}). The $T = 0$ energies serve as a kinetic obstacle against collapse, allowing metastable BEC to be formed if $A < A_{\mathrm{cr}}$ [32–36]. We think that, the study of $T = 0$ energies of BEC is an effective tool for exploring the

Published online: 13 July 2022

role of external confinement near the collapse of the system. In previous attempts, we studied the interaction energy (V_{int}), kinetic energy (T), trapping potential energy (V_{trap}) along with the total ground-state energy (E_0) of the attractive condensate [37,38]. But studies were limited to harmonic trapping case where the interaction between atoms was increased by increasing A, which causes the collapse of the BEC. However, in the practical situation of experiments, the trap usually is of finite extent. With this concern, the study of $T = 0$ energies of the attractive BEC in anharmonic trap is also important. In [24], the strength of the quartic confinement was $\lambda \simeq 10^{-3}$ and we also take the controllable anharmonic parameter as $|\lambda| \ll 1.0$. We keep increasing the strength of λ which causes the collapse of the condensate. We aim to study V_{int}, T, V_{trap}, E_0 of the attractive condensate as a function of λ for both laser blue-shifted ($\lambda > 0$) and laser red-shifted ($\lambda < 0$) anharmonic confinement. We also calculate the average root mean square radius (r_{av}) of the individual atoms from the centre of mass of the system [29], to get the idea of the average size of the condensate in anharmonic trap. It is observed that the system contracts with $\lambda > 0$ while it expands with $\lambda < 0$. The total ground-state energies are also modified accordingly. For a fixed number of particles (A), if we tune λ (keeping $\lambda \ll 0$), we observe that, both $\langle V_{\mathrm{trap}}\rangle/A$ and $\langle V_{\mathrm{int}}\rangle/A$ increase prominently with a sharp decrease of $\langle T\rangle/A$ in quadratic plus quartic confinement. The collapse of the attractive system is demonstrated by the decreasing nature of $\langle V_{\mathrm{trap}}\rangle/A$ and $\langle V_{\mathrm{int}}\rangle/A$ along with the increase in $\langle T\rangle/A$ when it is confined by the harmonic trap only [37,38]. Here, the present observation is distinctly different from earlier study for attractive BEC in a harmonic trap. The results are really dramatic and the metastable condensate is observed to be bounded by two neighbour barriers of different heights on two sides. On the left side of the left intermediate barrier (LIB), there is a deep narrow attractive well (NAW) which is the effect of negative scattering length as one gets for the attractive condensate in the usual case of harmonic trapping [37]. The right intermediate barrier (RIB) is the effect of negative value of anharmonicity which basically corresponds to finite optical trap. The RIB vanishes for $\lambda \geq 0$ and we observe that, the right side wall of the metastable region (MSR) in the outer part of the trap becomes stiff on increasing the strength of anharmonicity (λ). We again investigate the zero-point energies and observe that both $\langle V_{\mathrm{trap}}\rangle/A$, $\langle V_{\mathrm{int}}\rangle/A$ decrease with very tiny increase of λ which seduces the system towards collapse. Observations are interesting and the rate of change of $T = 0$ energies are significant for larger number of particles though the chosen value of scattering length is quite small. We find a critical value of anharmonicity (λ_{cr}) to collapse the metastable condensate. When $\lambda \geq \lambda_{\mathrm{cr}}$, the attractive interaction steers the trapping potential energy and makes the condensate unstable. We also tune λ very close to criticality and calculate the quantum tunnelling probabilities (P_t) of particles from the metastable condensate through the LIB into the inner core (NAW) near the origin. Results are impressive as P_t increases significantly on very little strengthening of λ. In the experiments of BEC with finite trap, the trapping potential is imposed optically by tuning of laser intensity as mentioned above and it controls the height of external potential. Tuning of λ in our study is corroborative with real experimental situation and thus significant from experimental point of view also.

The paper is organised as follows. In §2, we introduce the calculations that were used to find the zero-point energies and the tunnelling probabilities of a large number of trapped bosons. In §3, we discuss our results and finally §4 concludes the summary of our work. Throughout the present communication, energies are expressed in the oscillator unit (o.u.) of energy ($\hbar\omega$) and lengths are expressed in the o.u. of length ($a_{\mathrm{ho}} = \sqrt{\hbar/m\omega}$).

2. Methodology

The earlier theoretical studies to explain the gross physical properties of the BEC were well described by the Gross–Pitaeveskii (GP) equation. GP is basically a mean-field theory where the two-body interaction is assumed as a zero-range contact δ-interaction [39]. In this approximation, the total condensate wave function is taken as the product of single-particle wave functions and the effect of atomic correlation is completely ignored [40]. But the attractive condensate becomes highly correlated when the system is close to criticality, as the atoms come closer and closer. Two and higher body correlations play important roles in this high density regime. The theoretical method we adopt here is the potential harmonic expansion method (PHEM), which takes care of the effect of interatomic correlations. The theoretical formalism of PHEM was first adopted by Fabre de la Ripelle in 1986 and intended for nuclear systems consisting of fermions [41,42]. PHEM is actually an extension of the hyperspherical harmonic expansion method (HHEM), which is suitable for extremely dilute system and thus ideal to apply in BEC. This method is facilitated by the use of realistic two-body potentials (viz. van der Waals potential) and has already been established as a very useful technique to study the properties of BEC [17–19,29–31,43–46]. Here, we describe the methodology briefly for the interested readers. Details of the technique and explanation of the adopted notations and terminology can be found in mentioned references.

We consider a system of $A = (N+1)$ atoms (each of mass m) confined in an external trapping potential, $V_{\rm trap}$ (acting on each individual boson) and interacting via a two-body potential $V(\mathbf{x}_i - \mathbf{x}_j)$ for the (ij)-pair. The Hamiltonian for this system is

$$H = \sum_{i=1}^{A}\left(-\frac{\hbar^2}{2m}\nabla_i^2 + V_{\rm trap}(\mathbf{x}_i)\right) + \sum_{i>j=1}^{A} V(\mathbf{x}_i - \mathbf{x}_j). \quad (1)$$

In PHEM, the many-body wave function (ψ) is represented by a sum of all possible $[A(A-1)/2$ in number$]$ Faddeev-type decompositions,

$$\psi = \sum_{ij>i}^{N+1} \psi_{ij}. \quad (2)$$

The (ij)th Faddeev component (ψ_{ij}) corresponds to ith and jth particles interacting, while the rest $(A-2)$ particles are inert spectators. A realistic two-body interaction (van der Waals interaction) has been chosen to act between the interacting pair. Thus, each Faddeev component as well as the full wave function (ψ) involve all the coordinates of A particles. The Schrödinger equation for ψ_{ij} becomes

$$(T_k + V_{\rm trap} - E)\psi_{ij}(\mathbf{x}) = -V(\mathbf{r}_{ij}) \sum_{k,l>k}^{N+1} \psi_{kl}(\mathbf{x}), \quad (3)$$

T_k being the total kinetic energy operator, E is the total energy and $V(r_{ij})$ is the pairwise local central two-body interaction between the ith and jth particles, $\mathbf{r}_{ij} = \mathbf{x}_i - \mathbf{x}_j$. Next, a set of N Jacobi vectors are defined to remove the centre of mass motion [31]. According to the definition of Jacobi coordinates [41,47],

$$\boldsymbol{\zeta}_i = \left(\frac{2i}{i+1}\right)^{1/2}\left[\mathbf{x}_{i+1} - \frac{1}{i}\sum_{j=1}^{i}\mathbf{x}_j\right], \quad i = 1, 2, \ldots$$

and the centre of mass $\mathbf{R} = \frac{1}{A}\sum_{i=1}^{A}\mathbf{x}_i$. The relative motion after the removal of the centre of mass motion is described by [41]

$$\left[-\frac{\hbar^2}{m}\sum_{i=1}^{N}\nabla_{\zeta_i}^2 + \sum_{i=1}^{N}\left(\frac{1}{2}m\omega^2\zeta_i^2 + \lambda\zeta_i^4\right) + V_{\rm int}\right]\psi = E_R\psi(\boldsymbol{\zeta}_1, \ldots, \boldsymbol{\zeta}_N). \quad (4)$$

Here we assume that the system is confined by quadratic plus quartic-type anharmonic potential. $V_{\rm int}$ is the sum of all pairwise interactions and E_R is the energy of the relative motion ($=E-$ centre of mass energy). Next, let us consider the hyperspherical variables which are constituted by the hyper-radius (r) and $(3N-1)$ 'hyperangles' consisting of $2N$ spherical polar angles of $\{\zeta_1, \zeta_2, \ldots, \zeta_{\rm N}\}$ and $(N-1)$ hyperangles $\{\phi_2, \ldots, \phi_N\}$ (with associated quantum numbers $\{n_2, \ldots, n_N\}$) giving the relative lengths of N Jacobi vectors. In this choice, the $3N$-dimensional Laplace operator can be split into the hyper-radial plus the hyper-centrifugal kinetic energy (KE) terms.

$$\nabla^2 \equiv \sum_{i=1}^{N}\nabla_{\zeta_i}^2 = \frac{\partial^2}{\partial r^2} + \frac{3A-4}{r}\frac{\partial}{\partial r} + \frac{L^2(\Omega_N)}{r^2}, \quad (5)$$

where Ω_N is an abbreviation for the set of $(3N-1)$ hyperangles and $L^2(\Omega_N)$ is the grand orbital operator in $3N$ dimensional space. Since for the (ij) Faddeev component the $(N-1)$ inert particles do not interact, they contribute only to the total KE. Also note that ψ_{ij}, which corresponds to (ij) interacting pair, is a function of the pair separation $\mathbf{r}_{ij}$ and the global hyper-radius r. We expand ψ_{ij} in a subset of the full hyperspherical basis, called potential harmonic (PH) basis [30,31]. It is noteworthy to mention that, the inertness of particles allows the (ij) Faddeev component ψ_{ij} to be expanded in the PH basis.

$$\psi_{ij} = r^{-(\frac{3N-1}{2})}\sum_K \mathcal{P}_{2K+l}^{lm}(\Omega_N^{(ij)})u_K^l(r)\eta(r_{ij}). \quad (6)$$

$\mathcal{P}_{2K+l}^{lm}(\Omega_N^{(ij)})$ is a PH basis function and $\Omega_N^{(ij)}$ is the set of all hyperangles for the choice $\boldsymbol{\zeta}_N \propto \mathbf{r}_{ij}$. Here, we introduce $\eta(r_{ij})$ as a short-range correlation function in each Faddeev-type component which properly simulates the short separation behaviour of an interacting pair. We obtain $\eta(r_{ij})$ as the zero energy solution of the (ij)-pair relative motion in the potential $V(\mathbf{r}_{ij})$ [29,45].

$$-\frac{\hbar^2}{m}\frac{1}{r_{ij}^2}\frac{\mathrm{d}}{\mathrm{d}r_{ij}}\left(r_{ij}^2\frac{\mathrm{d}\eta(r_{ij})}{\mathrm{d}r_{ij}}\right) + V(r_{ij})\eta(r_{ij}) = 0. \quad (7)$$

The correlation function quickly attains its asymptotic form $C(1-\frac{a_{\rm sc}}{r_{ij}})$ for large r_{ij}. The asymptotic normalisation is chosen to make the wave function positive at large r_{ij} [29]. The need for such a correlation function can also be understood from the experimental context. In a typical BEC experiment, the condensate is kept at a very low temperature and in very dilute condition. Hence, only binary collision at almost zero kinetic energy is relevant, which is completely described in terms of the s-wave scattering length. The PH basis set will not contain any function of the corresponding $\boldsymbol{\zeta}_k$ with $k < N$ and is given (for the ij-interacting pair, such that $\boldsymbol{\zeta}_N \propto \mathbf{r}_{ij}$) by [41,42]

$$\mathcal{P}^{l,m}_{2K+l}(\Omega^{(ij)}_N) = Y^m_l(\omega_{ij})\ {}^{(N)}P^{l,0}_{2K+l}(\phi)\mathcal{Y}_0(3N-3), \tag{8}$$

the wave function of the $(N-1)$ inert particles being $\mathcal{Y}_0(3N-3)$ which is basically the hyperspherical harmonic (HH) of order zero in the $(3N-3)$-dimensional space, spanned by the vectors $(\boldsymbol{\zeta}_1, \ldots, \boldsymbol{\zeta}_{N-1})$ and ϕ is the hyperangle given by $r_{ij} = r\cos\phi$. Note that, PHs are the eigenfunctions of $L^2(\Omega_N)$

$$\left[L^2(\Omega_N) + \mathcal{L}(\mathcal{L}+3N-2)\right]\mathcal{P}^{l,m}_{2K+l}(\Omega^{(ij)}_N) = 0, \tag{9}$$

where $\mathcal{L} = 2K + 1$ and in choosing the PH basis, we assume that the inert particles are in their lowest hyperangular state and do not contribute to the hyperangular momentum. The sole contribution to the latter comes from the interacting pair. The PH basis is a subset of HH basis having special restrictive values of the $(3N-1)$ quantum numbers

$$\begin{aligned} &l_1 = l_2 = \cdots = l_{N-1} = 0, l_N = l \\ &m_1 = m_2 = \cdots = m_{N-1} = 0, m_N = m \\ &n_2 = n_3 = \cdots = n_{N-1} = 0, n_N = K \end{aligned} \tag{10}$$

such that the orbital and grand orbital of the system is contributed by the interacting pair alone. This effectively corresponds to the inclusion of only two-body correlations in each Faddeev-type component (associated with the interacting pair) of the wave function ψ. Thus, for any N corresponding to three degrees of freedom of the relative separation vector of the interacting pair, there are only three independent quantum numbers $(2K + l, l, m)$. This assumption is justified by the fact that in a BEC, almost all the particles are in their lowest energy state. Indeed, this is the basic assumption of this method (the other assumption that only two-body interactions are relevant is quite intuitive).

Counting the degrees of freedom (number of variables of the wave function): The relative wave function after removing the centre of mass motion of an A particle system involves $3N$ variables, where $N = A - 1$. Both the full (relative) wave function ψ and the (ij) Faddeev component ψ_{ij} of eq. (2) involve $3N$ variables. This can be seen from eq. (6), in which the potential harmonic $\mathcal{P}^{lm}_{2K+l}(\Omega^{(ij)}_N)$ involves $(3N-1)$ variables and the global hyper-radius r is one, making up a total of $3N$ variables. Note that, r_{ij} is not an independent variable as it is proportional to ζ_N. We can see from eq. (8) that the PH involves $(3N-1)$ variables, consisting of $Y^m_l(\omega_{ij})$ has two, ${}^{(N)}P^{l,0}_{2K+l}(\phi)$ has one and $\mathcal{Y}_0(3N-3)$ has $(3N-4)$ hyperangles (excluding the corresponding hyper-radius). The integrations over volume elements (which do not appear explicitly in the paper) are also correct for the $3N$-dimensional space (see refs [41,47]).

The final equation [eq. (11)] is obtained by integrating the over all $(3N-1)$ hyperangles, after multiplying by complex conjugate of the full HH [i.e., projecting the full Schrödinger equation on the hyper-radial (r) space]. The interaction potential term gives rise to the coupling term involving $V_{KK'}(r)$. Note that, $\mathcal{Y}_0(3N-3)$ (which is a constant) is already normalised over $(3N-4)$ corresponding hyperangles [47].

$$\begin{aligned} &\left(-\frac{\hbar^2}{m}\frac{\mathrm{d}^2}{\mathrm{d}r^2} + V_{\text{trap}} - E_R\right)U_{Kl}(r) \\ &\quad + \frac{\hbar^2}{mr^2}\left\{4K(K+\alpha+\beta+1) + \overline{\mathcal{L}}(\overline{\mathcal{L}}+1)\right\}U_{Kl}(r) \\ &\quad + \sum_{K'} f_{Kl}V_{KK'}(r)f_{K'l}U_{K'l}(r) = 0, \end{aligned} \tag{11}$$

where $V_{\text{trap}} = \frac{1}{2}m\omega^2r^2 + \lambda r^4$ is the externally applied trapping potential.

$$\begin{aligned} &U_{Kl}(r) = f_{Kl}(h^{\alpha\beta}_K)^{\frac{1}{2}}u^l_K(r), \\ &\overline{\mathcal{L}} = l + \frac{3A-6}{2}, \alpha = \frac{3A-8}{2}, \beta = l + \frac{1}{2}, \end{aligned}$$

f_{Kl} is a constant representing the overlap of the PH for interacting partition with the full set, which is given in ref. [41]. The Schrödinger equation for the (ij) Fadeev component thus becomes a differential equation in $\mathbf{r}_{ij}$ variable only, with an effective interaction. Because of the fact that all the particles are identical, one can drop the label ij also. The potential matrix element $V_{KK'}(r)$ is given by

$$\begin{aligned} V_{KK'}(r) &= \frac{1}{\sqrt{(h^{\alpha\beta}_K h^{\alpha\beta}_{K'})}}\int_{-1}^{+1} P^{\alpha\beta}_K(z)V\left(r_{ij}\right) \\ &\quad \times P^{\alpha\beta}_{K'}(z)\eta\left(r_{ij}\right)W_l(z)\mathrm{d}z\cdot \end{aligned} \tag{12}$$

Here, $h^{\alpha\beta}_K$ and $W_l(z)$ are respectively the norm and weight function of the Jacobi polynomial $P^{\alpha\beta}_K(z)$ and $r_{ij} = r\sqrt{(1+z)/2}$ [48]. So, the numerical difficulty in the imposition of symmetry and calculation of potential matrix becomes tremendously simplified as $(3N-1)$ hyperspherical angle variables are reduced effectively to only three active 'angle' variables for any N. The Schrödinger equation is also simplified enormously; it becomes a two-body equation for any A. As mentioned above, this is possible due to two assumptions: (1) While two particles interact, the rest of the particles are only spectators and do not contribute to the potential energy or to the hyperangular momenta. This assumption is very well justified for the BEC. BEC is experimentally achieved in an extremely dilute atomic gas at an extremely low temperature, conditions necessary to avoid the formation of molecules and clusters from the atoms (which will deplete the BEC). The choice of the PH basis is manifestly justified, and by definition the ideal BE condensate occurs when all the atoms (bosons) are in their lowest energy states and (2) only two-body interactions are relevant. This assumption is again fully justified for the extremely dilute BEC, for which the probability of more than two particles coming within the range of force is completely negligible. Naturally, PHEM will not be applicable for a denser system. The PHEM has an important advantage: it can incorporate a realistic 2-body interaction. It is also important to note that our correlated basis function keeps all possible two-body correlations. However, one has to ascertain the contribution of the disregarded higher than two-body correlations. In spite of this, PHEM is a very effective tool for investigating BEC as the condensed system is extremely dilute.

3. Results and discussion

3.1 *Choice of interatomic potential*

In our present calculation, we model the interatomic interaction by a realistic long-range potential, the van der Waals potential with a hard core of radius r_c, viz., $V(r_{ij}) = \infty$ for $r_{ij} \leq r_c$ and $= -(C_6/r_{ij}^6)$ for $r_{ij} > r_c$. C_6 is known for a specific atom and for Rb atoms, $C_6 = 6.4898 \times 10^{-11}$ o.u. [49]. The value of r_c is adjusted to get the desired value of $a_{\rm sc}$ [49]. In the limit of $C_6 \to 0$, the potential becomes a hard core potential and r_c coincides with the s-wave scattering length $a_{\rm sc}$. However, with a $1/r^6$ tail, we have to solve the two-body Schrödinger equation with zero energy to get the value of r_c, which corresponds to the experimental scattering length $a_{\rm sc}$. With a tiny change in r_c, $a_{\rm sc}$ may even change sign [49]. Thus, the choice of r_c is very crucial. For attractive BEC, the $a_{\rm sc}$ values as reported in the controlled collapse experiment of ^{85}Rb atoms [26–28]. The required values of r_c are determined and presented in our previous work [38]. The chosen parameter for our present calculation is $r_c = 1.3955 \times 10^{-3}$ o.u. With these set of parameters we solve the coupled differential equation by hyperspherical adiabatic approximation (HAA) [50]. We diagonalise the potential matrix together with hypercentrifugal repulsion and obtain the lowest eigenpotential $\omega_0(r)$. We consider collective motion of the condensate in the effective many-body potential $\omega_0(r)$ in hyper-radial space in which the condensate moves collectively. The energy and wave function of the condensate are finally obtained by solving the adiabatically separated hyper-radial equation which is given by

$$\left[-\frac{\hbar^2}{m}\frac{\mathrm{d}^2}{\mathrm{d}r^2} + \omega_0(r) - E_R\right]\zeta_0(r) = 0, \quad (13)$$

subject to approximate boundary condition on $\zeta_0(r)$. For our numerical calculation, we fix $l = 0$ and truncate the correlated PH basis to a maximum value $K = K_{\rm max}$ requiring proper convergence [30].

3.2 *Attractive condensate confined in harmonic trap ($\lambda = 0$)*

The many-body effective potentials ($\omega_0(r)$) for the attractive condensate, confined in the harmonic trap is plotted in panels 1 and 2 of figure 1. The MSR of $\omega_0(r)$ basically holds the condensate. The MSR is bounded on the right side by a high wall of the external harmonic trap and on the left by the LIB. The latter exists due to the negative scattering length. On the left of LIB, a very deep but finite NAW appears which is again followed by a steeply increasing repulsive wall as r decreases (panel 1). We obtain this strong repulsive core near the origin ($r \to 0$) due to the use of realistic van der Waals interaction in quantum many-body calculation. If the number of atom increases, the height of the LIB decreases and minimum of MSR increases (panel 2). At a critical value of A ($= A_{\rm cr}$), the local maximum of LIB and the minimum of MSR coincide to form a point of inflexion, with the disappearance of the MSR [37,45]. All atoms get trapped by the attractive inner core (NAW) then, giving rise to cluster state resulting from the increased interatomic correlation. The release of binding energy is observed as a burst of energy in experiments. The obtained critical number of ^{85}Rb condensate with $a_{\rm sc} = -1.832 \times 10^{-4}$ o.u. by our many-body theory is 2484 [38] while the experimental value is 2500 [26]. The total energy per particle (E_0/A) in MSR decreases gradually with the increase of A due to the accumulation of particles in NAW [37,38,45]. To get a more clear idea, we study the average size of the condensate ($r_{\rm av}$), which is defined as the root mean square (rms) distance of individual atoms from the centre of mass.

$$r_{\rm av} = \left\langle \frac{1}{A}\sum_{i=1}^{A}(\mathbf{x}_i - \mathbf{X})^2 \right\rangle^{1/2} = \frac{\langle r^2\rangle^{1/2}}{\sqrt{2A}}. \quad (14)$$

The last step in eq. (12) follows from the definition of the hyper-radius r [41] and $\mathbf{X}$ is the centre of mass coordinate. In table 1, we present the obtained value of E_0/A, $r_{\rm av}$ for different number of bosons. With increase in particle number, the total attractive interaction increases as $[A(A-1)]/2$, the system contracts and $r_{\rm av}$ decreases

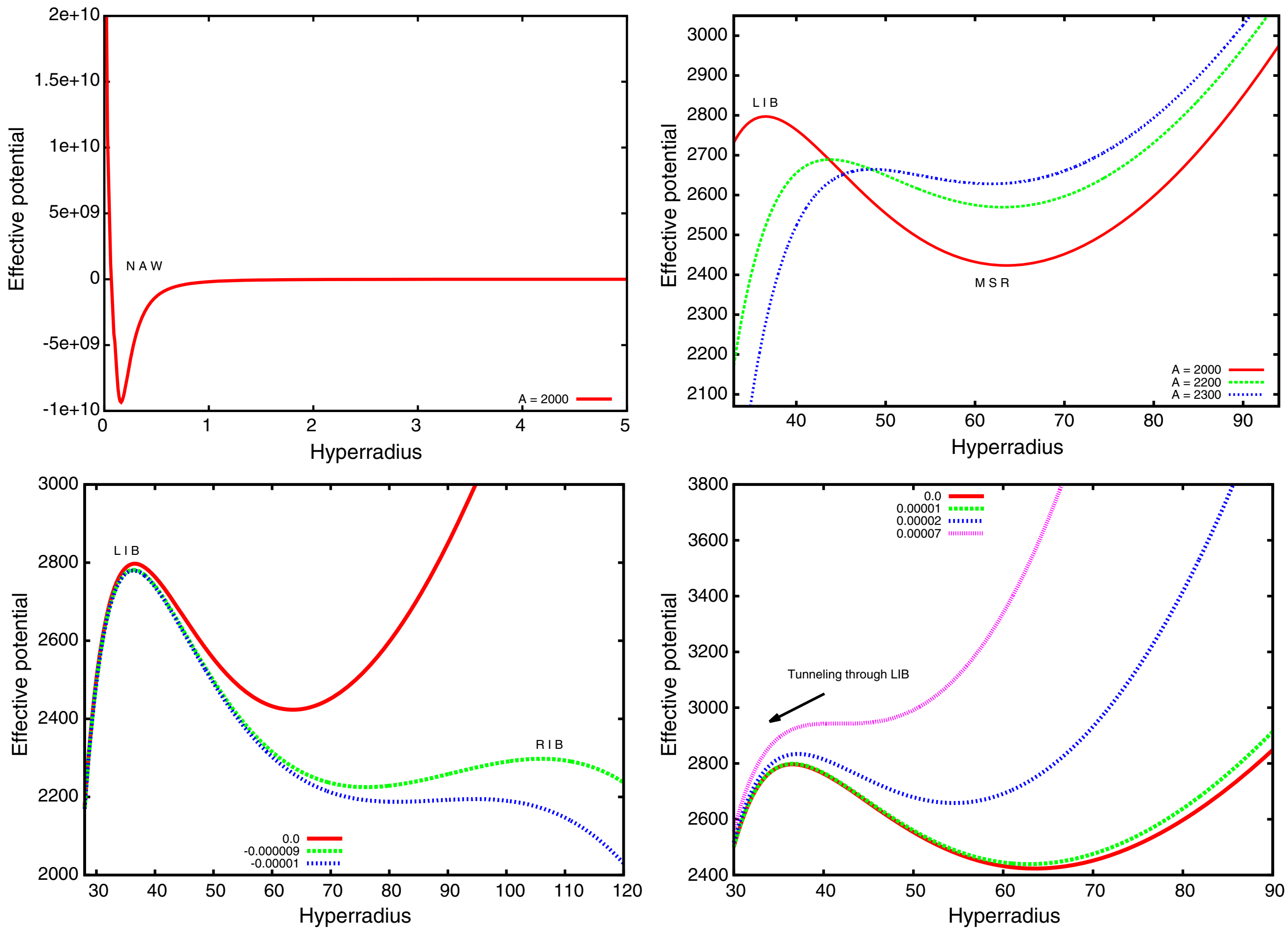

Figure 1. Plot of effective potential ($\omega_0(r)$) in o.u. against r (o.u.) of ^{85}Rb atoms with scattering length $a_{\rm sc} = -1.832 \times 10^{-4}$ o.u. The first two panels are plotted by considering harmonic trap potential ($\lambda = 0$). In panel 1, the deep NAW is plotted for $A = 2000$, while panel 2 displays the MSR in details for $A = 2000$, 2200 and 2300. The tunnelling picture of the condensate through the LIB by increasing A, is clear from this panel. The third and fourth panels show $\omega_0(r)$ when the condensate is confined by anharmonic trap $V(r) = \frac{1}{2}m\omega^2 r^2 + \lambda r^4$, with different values of anharmonic coefficient (λ) as indicated in figures for $A = 2000$. When $\lambda < 0$, the metastability is different (panel 3) and the condensate suffers significant tunnelling through the RIB also, when strength of λ enhances slightly. Panel 4 demonstrates the modelling of $\omega_0(r)$ on increasing the strength of λ (keeping $\lambda \geq 0$). The condensate tunnels through LIB only into the inner core (NAW) and at a critical value of λ ($= \lambda_{\rm cr}$), the MSR disappears. A very weak MSR is also shown when the condensate is confined by an anharmonic trap for $\lambda = 7.0 \times 10^{-5}$ (very close to $\lambda_{\rm cr}$). Note the different horizontal and vertical scales of the first panel.

as expected. We also present the result from the GP equation method in the same table. The GP equation method is basically a mean-field theory where the two-body interaction is assumed to be a zero-range contact interaction only. It gives a fairly good description of BEC. In the present method, we incorporate realistic van der Waals potential and consider two-body correlation which lowers the energy. Note that the energy per particle by the PHEM is less than the GP value. It is also seen that the obtained value of average size of the condensate by our many-body method are not in very close agreement with those calculated from the GP equation.

Table 1. Calculated values of ground-state energy per atom (E_0/A) (in o.u.) and average size of the condensate (in o.u.) for different A of ^{85}Rb condensate with scattering length $a_{sc} = -1.8322 \times 10^{-4}$ o.u. Results of both many-body theory (PHEM) and GP equation method are presented.

A	$(E_0/A)_{\rm PHEM}$	$(E_0/A)_{\rm GP}$	$(r_{\rm av})_{\rm PHEM}$	$(r_{\rm rms})_{\rm GP}$
10	1.51543	1.51501	1.17115	1.2354
100	1.47370	1.49263	1.21167	1.7296
500	1.44143	1.46209	1.18964	1.7058
1000	1.37643	1.42119	1.15400	1.6749
2000	1.21289	1.32645	1.00448	1.5909

3.3 *Attractive condensate confined in anharmonic trap with* $\lambda < 0$

We now consider the attractive condensate which is confined in quadratic plus quartic trap with $\lambda \ll 0$ and drastic effects are seen in remodelling the outer part of the trap. In experiments [24,25], the height of the potential well was controlled by adjusting the laser intensity in the optical trap. In our study, we tune λ in a controlled fashion to observe the important role of quartic term to modify the MSR. The notable effect due to anharmonicity is clear from panel 3 of figure 1, where $\omega_0(r)$ is plotted for $A = 2000$ with $\lambda = 0, -9\times 10^{-6}$ and -1×10^{-5}. The metastable condensate is now bounded by an additional neighbour barrier on the right side of MSR. This right intermediate barrier (RIB) is the effect of negative anharmonicity and basically corresponds to finite optical trap. Naturally, in such a situation, the MSR becomes flattened and condensate will have the probability to tunnel out the trap through both the barriers. We have checked that with a very week anharmonicity ($\lambda \simeq -1.2 \times 10^{-5}$), the barrier on the right side quickly decreases even when A (= 2000) is quite smaller than $A_{\rm cr}$ ($\simeq$ 2500, experimentally).

We calculate several ground-state properties in different metastabilities, the trap energy ($\langle V_{\rm trap}\rangle = \langle \sum_{i=1}^{A} [\frac{1}{2}m\omega^2 {r_i}^2 + \lambda {r_i}^4]\rangle$), the interaction energy ($\langle V_{\rm int}\rangle = \langle \sum_{i,j<i}^{A} V_{ij}\rangle$), kinetic energy ($\langle T\rangle$), the total ground-state energy (E_0) of the condensate to explore the role of anharmonicity. The expectation value of trap energy per particle ($\langle V_{\rm trap}\rangle/A$) is plotted in figure 2 as a function of the anharmonic parameter λ, for 1000, 1500 and 2000 number of bosons. In our many-body method, the effective potential $\omega_0(r)$ has a large contribution from the trapping potential and it decreases gradually at smaller values of r, where NAW is located. In the usual case of attractive condensate by harmonic trapping, we observed that, $\langle V_{\rm trap}\rangle/A$ decreases gradually as A increases and finally the condensate collapses [37,38]. But in the present study, collapse is accomplished by very slight tuning of λ towards strong anharmonicity (still $-2\times 10^{-5} < \lambda < 0$). We see a prominent increase of $\langle V_{\rm trap}\rangle/A$ with increase in $|\lambda|$. The rate of increase is more significant for larger number of particles though the chosen value of scattering length is quite small. The result is interesting as the increase of $\langle V_{\rm trap}\rangle/A$ gives the collapse scenario of the condensate here. The observation has dissimilarity with our previous study but it is expected, since the effective potential well becomes flattened due to rapid growth of the quartic term of the potential in higher r region and MSR of the condensate expands.

The expansion of the MSR of the condensate will be more clear from figure 3, where the dependency of $r_{\rm av}$ on λ is displayed for A =1000, 1500 and 2000. We observed a considerable decrease of $r_{\rm av}$ with increase of A in pure harmonic well [37,38], where the MSR is bounded only by LIB and right side of the well increases sharply. Since the total attraction between atoms increases rapidly as the number of binary bonds increases with A, this causes the decrease in height of LIB. The effect tends toward the collapse of the system and the condensate will decay only through the LIB near the origin forming bound clusters of atoms. But the role of anharmonicity is to pull down the height of MSR in higher r region (figure 1, panel 3). This is a very interesting situation when the condensate in the MSR is bounded by two barriers (LIB and RIB) of finite

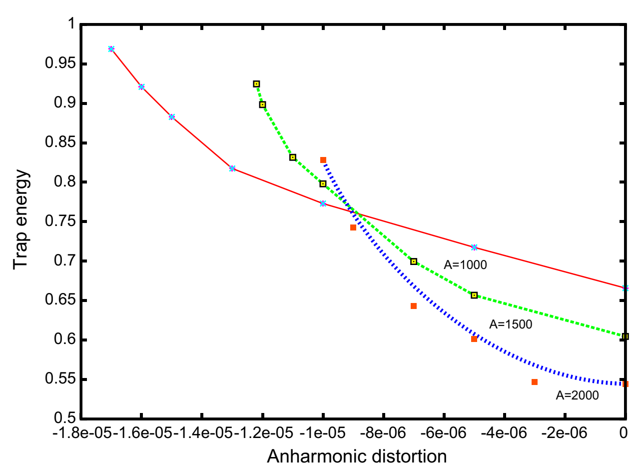

Figure 2. Plot of the trapping potential energy per particle $\langle V_{\rm trap}\rangle/A$ (o.u.) as a function of anharmonicity λ, for different indicated values of A.

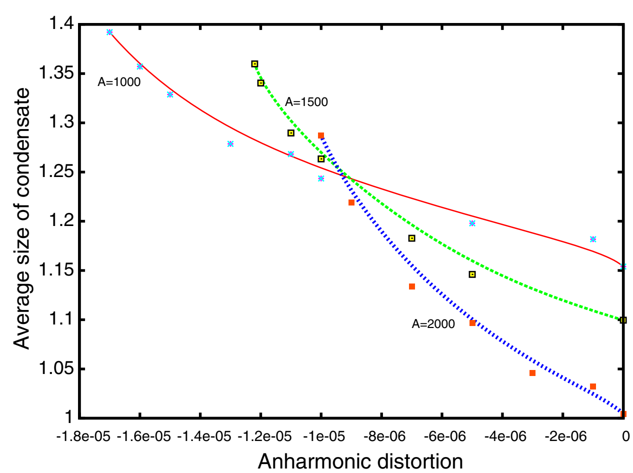

Figure 3. Plot of the average size of the condensate $r_{\rm av}$ (o.u.) as a function of anharmonicity λ, for different indicated values of A.

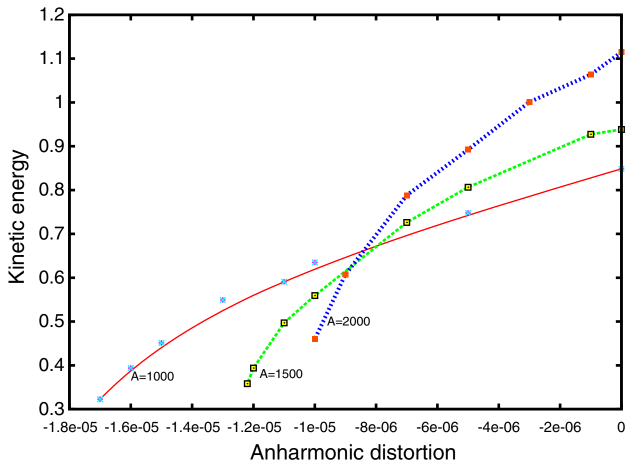

Figure 4. Plot of kinetic energy per particle ($\langle T \rangle / A$) in o.u. as a function of anharmonicity λ, for different indicated values of A.

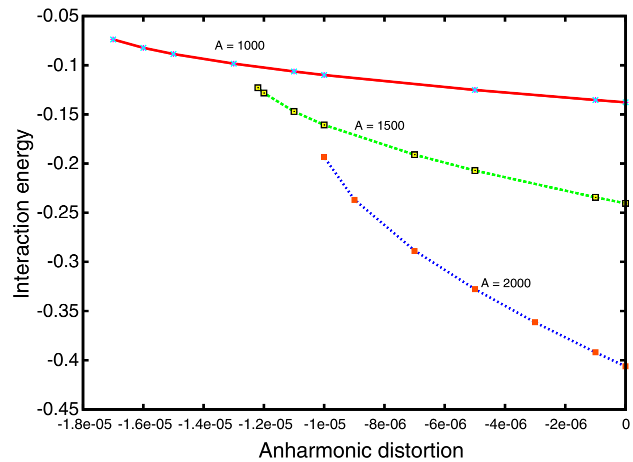

Figure 5. Plot of interaction energy per particle ($\langle V_{\text{int}} \rangle / A$) in o.u. as a function of anharmonicity λ, for different indicated values of A.

width and may suffer tunnelling through both the barriers simultaneously. Due to the very less contribution of the quartic term of the trapping potential near $r \to 0$, the height of the LIB remains almost the same for all values of λ. But the height of the RIB decreases very quickly and $\omega_0(r)$ becomes less stiff (compared with harmonic trapping) on very small increase of λ. If the strength of λ is increased more (still $|\lambda| \leq 10^{-6}$), the height of RIB turns smaller than the height of LIB and transmission probability through the RIB sets to high compared to that through LIB. But this time there will be no cluster formation; the atoms will escape outwards from the metastable trap and form a dilute non-condensed Bose gas by tunnelling through RIB. Thus, we fail to get a permanently stable condensate for all values of λ. So, the sharp increase of r_{av} in flattened well with the increase in λ is again expected but it does not tend to the increase of stability of the condensate.

We next study the modification of kinetic energy and interaction energy of the attractive condensate by tuning the coefficient of quartic term (λ). The obtained interaction energy $\langle V_{\text{int}} \rangle$ is always negative due to the effective attractive interaction ($a_{\text{sc}} < 0$) and becomes more negative with increase in the number of atoms (A). But, in anharmonic well for fixed A, tunnelling of the condensate through RIB increases on increasing the strength of λ, as stated earlier. The effect is again impressive as it leads to a considerable decrease of $\langle T \rangle$ and as an immediate result, $\langle V_{\text{int}} \rangle$ becomes less negative. This development is expected to enhance for larger A. We plot $\langle T \rangle / A$ as a function of λ for A=1000, 1500, 2000 in figure 4 and $\langle V_{\text{int}} \rangle / A$ is plotted as a function of λ in figure 5. After the collapse of the attractive BEC with harmonic trapping [37,38], the system tunnels inwards through LIB only into the NAW and crumbling of the

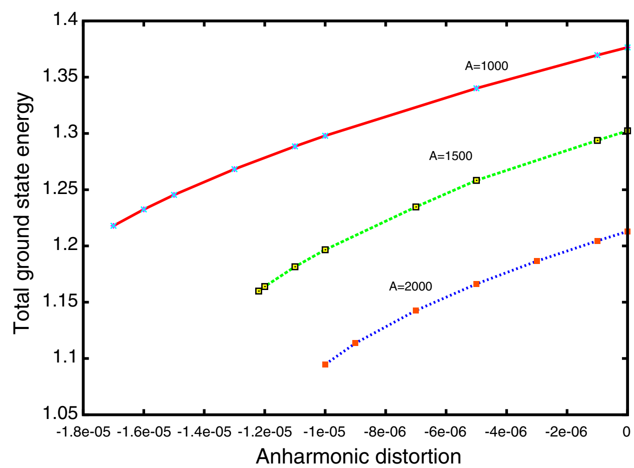

Figure 6. Plot of ground-state energy per particle ($\langle E_0 \rangle / A$) in o.u. as a function of negative anharmonicity λ, for different indicated values of A.

condensate is attributed by a sharp increase of $\langle T \rangle / A$ with a notable decrease of $\langle V_{\text{int}} \rangle / A$. But, our present investigation with anharmonic trapping is in sharp contrast with the previous observations as a significant fall of $\langle T \rangle / A$ with a considerable increase of $\langle V_{\text{int}} \rangle / A$ gives a signature of the collapse of the condensate. Results are more interesting when we take a look at the total ground-state energy (E_0) per atom. We display it as a function of λ in figure 6. The gradual decrease in E_0 / A with a very little strengthening of λ, instigates the system towards collapse and the finding is in good agreement with the earlier results [37,38].

The study of wave function of the trapped condensate is also a subject of great interest as one gets the knowledge of density profile of the system in the presence of the anharmonic trap. The stable wave functions

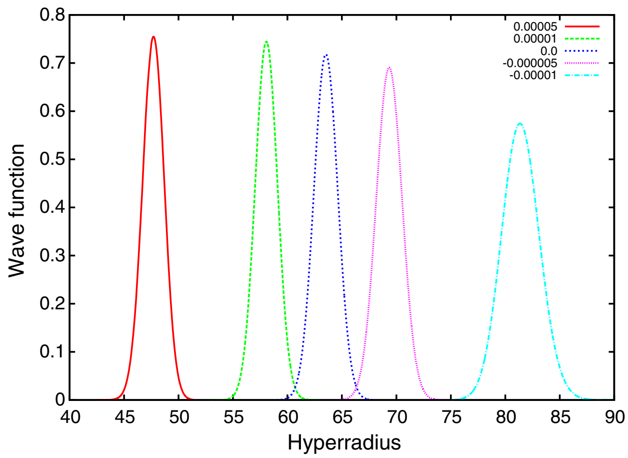

Figure 7. Plot of ground-state wave function as a function of hyper-radius r (o.u.) for 2000 trapped particles with different indicated values of anharmonicity (λ).

for a metastable condensate ($A = 2000$) as a function of the hyper-radius (r) are presented in figure 7 for different values of anharmonicity (λ). The wave function is centred at the MSR minimum of $\omega_0(r)$. It is seen that, as the strength of anharmonicity increases (keeping $\lambda < 0$), the peak of the wave function shifts towards larger values of r. This is understandable, since for flattened many-body effective potential well, particles are allowed to go outwards through RIB. The hyper-radial space in which the condensate moves, increases.

3.4 *Attractive condensate confined in anharmonic trap with $\lambda > 0$*

Next, we study the $T = 0$ ground-state properties of ^{85}Rb condensate by considering positive values of anharmonic term (λ). We again keep increasing λ very slowly and observe very prominent effect of anharmonicity as this causes the upward shift of the whole effective potential. It is noticed that, the effect of increasing λ for a fixed A, is to raise the minimum of MSR more compared with the peak of LIB (figure 1, panel 4). It reduces the depth of the MSR well and the MSR gradually shrinks also. The stability of the condensate decreases until a critical value of λ ($\lambda_{\rm cr}$) is reached. At $\lambda = \lambda_{\rm cr}$, the LIB and the minimum of MSR fuse to produce a point of inflection with simultaneous disappearance of the MSR. The deflationary effect of the MSR is also reflected in figure 7, where the wave function shifts towards smaller value of r as λ increases. This time, the condensate tunnels through the LIB only into the inner core (NAW) near the origin to form a bound cluster. A very weak MSR of 2000 trapped atoms, created by λ ($= 7.0 \times 10^{-5}$, very close to $\lambda_{\rm cr}$) is also shown in panel 4 of figure 1. The catching observation which appears in this analysis is $\lambda_{\rm cr}$. We find values of $\lambda_{\rm cr}$ which are 1.792×10^{-2} and 7.063×10^{-5} for $A = 1000$ and $A = 2000$, respectively.

Table 2. Calculated values of tunnelling probabilities (P_t) of atoms from the metastable region through the left intermediate barrier for different values of anharmonicity (λ) for fixed number of bosons (A).

A	Distortion (λ)	P_t
1000	1.65×10^{-2}	5.7140×10^{-5}
	1.66×10^{-2}	3.2757×10^{-4}
	1.67×10^{-2}	3.8728×10^{-4}
	1.68×10^{-2}	1.0257×10^{-3}
	1.69×10^{-2}	5.3830×10^{-3}
	1.70×10^{-2}	1.2672×10^{-2}
	1.71×10^{-2}	4.2356×10^{-2}
	1.72×10^{-2}	3.5586×10^{-1}
2000	6.30×10^{-5}	3.8697×10^{-8}
	6.35×10^{-5}	5.7043×10^{-6}
	6.40×10^{-5}	1.0768×10^{-5}
	6.45×10^{-5}	5.9312×10^{-5}
	6.50×10^{-5}	1.8485×10^{-4}
	6.55×10^{-5}	1.2698×10^{-3}
	6.60×10^{-5}	9.2509×10^{-3}
	6.65×10^{-5}	5.0766×10^{-1}

We turn now to the tunnelling of the metastable condensate through LIB into the NAW. We calculate the WKB tunnelling probability (P_t) of atoms from the MSR, to see how it changes on increasing the value of λ. The tunnelling probability is calculated as

$$P_t = \exp\left(-2 \int_{r_1}^{r_2} \sqrt{2[\omega_0(r) - E_0]}\, {\rm d}r \right), \qquad (15)$$

where r_1 and r_2 are the inner and outer turning points of the LIB of effective potential. In table 2, the obtained values of P_t are presented for different values of anharmonicity (λ) near its critical value for $A = 1000, 2000$. Near the criticality $\lambda \simeq \lambda_{\rm cr}$, the macroscopic tunnelling is quite high and increases significantly with increasing λ.

Let us now examine the behaviour of the $T = 0$ energies of the condensate with modelled external trapping potential. We consider that fixed number of atoms (A) are trapped by the anharmonic potential and our calculated expectation values of $V_{\rm trap}/A$, $V_{\rm int}/A$, T/A along with E_0/A and $r_{\rm av}$ are presented in table 3, for various values of λ. Note that, with increasing anharmonicity, $r_{\rm av}$ becomes lower which clearly signifies the gradual shrinking of the MSR. As λ increases, $\omega_0(r)$ grows more steeply for larger r which propels the system to tunnel inwards through LIB into the inner core (NAW) near the origin. The increase in $|\langle V_{\rm int}\rangle/A|$ and $\langle T\rangle/A$

Table 3. Calculated values of ground-state energy (E_0) per atom, trapping potential energy $\langle V_{\mathrm{trap}} \rangle$ per atom, interaction energy $\langle V_{\mathrm{int}} \rangle$ per atom, kinetic energy $\langle T \rangle$ per atom and average size of the condensate r_{av} for different values of anharmonicity (λ). We consider that fixed number of atoms (A) of ^{85}Rb condensate with scattering length $a_{\mathrm{sc}} = -1.8322 \times 10^{-4}$ are confined by anharmonic trapping potential. All the values are in oscillator unit.

A	Distortion (λ)	$\langle E_0 \rangle / A$	$\langle V_{\mathrm{trap}} \rangle / A$	$\langle V_{\mathrm{int}} \rangle / A$	$\langle T \rangle / A$	r_{av}
1000	0.0	1.376435	0.66586	−0.13776	0.84833	1.15400
	1.0×10^{-5}	1.43829	0.61114	−0.15881	0.98596	1.10557
	5.0×10^{-5}	1.61690	0.48915	−0.21985	1.34759	0.98909
	1.0×10^{-4}	1.77299	0.42723	−0.27602	1.62178	0.92437
	5.0×10^{-4}	2.41369	0.26569	−0.55076	2.69866	0.72897
	1.0×10^{-3}	2.83764	0.21425	−1.01333	3.63672	0.65461
2000	0.0	1.21290	0.54449	−0.40634	1.11474	1.00449
	1.0×10^{-5}	1.28040	0.42148	−0.53214	1.39107	0.91812
	2.0×10^{-5}	1.33039	0.37148	−0.64315	1.60207	0.86195
	5.0×10^{-5}	1.43066	0.28438	−0.97897	2.12526	0.75416

is due to the accumulation of atoms from MSR into the NAW. This is the collapse scenario in our approach which is accomplished by increasing the strength of λ. The picture is qualitatively the same as observed for the attractive BEC in our previous study [37,38]. However, the process to achieve collapse is a bit different from the commonly observed collapse of the attractive BEC in harmonic trap. In the latter case, the number of particle was increased for the condensate to emerge. It is important to point out that, we observe an acute increase of $\langle E_0 \rangle / A$ during the collapse of the condensate. It is in sharp contrast to the result of the attractive BEC in the harmonic trap. Although the observation is dramatic, it is understandable. As we have said earlier, our many-body effective potential shifts upwards as a whole as λ increases which causes the lifting of total ground-state energy (E_0). Our discussed collapsing nature of the attractive condensate depends strongly on the choice of interaction and number of trapped particle. The present study considers only a particular choice of scattering length and certain number of particles. So, further study with other experimental scattering lengths with a large number of particles is essential.

4. Summary and conclusions

In the present communication, we have considered an attractive Bose–Einstein condensed gas of ^{85}Rb atoms of the JILA experiment. The trapping potential is taken as the sum of a quadratic plus a quartic term, which approximates a harmonic confinement combined with a Gaussian envelope. We employ a method called potential harmonic expansion method (PHEM), where two-body correlations are taken into account and higher-order correlations are ignored. Since the experimental condensate is extremely dilute, the assumption is justified. Naturally, PHEM is not applicable for denser systems. This method can handle a realistic, finite-ranged interatomic interaction. We use the standard van der Waals potential with a hard core, reproducing the experimental s-wave scattering length. Main attention has been paid in the study of instability of the condensate when the effective trap height is tuned from harmonic to very weak anharmonicity. The coefficient of the quartic term (λ) has both positive and negative values. The deviation of the properties of BEC caused by anharmonic distortion is revealed and found to be more dramatic in the presence of atomic interaction. The situation is very interesting for red-shifted anharmonic trap ($\lambda < 0$), as the intermediate MSR is bounded by two neighbouring barriers. The right intermediate barrier (RIB) is the effect of negative anharmonicity which basically corresponds to a finite optical trap, whereas the left intermediate barrier (LIB) is the effect of negative a_{sc}. We observe the factors on which the heights of two barriers depend: λ and A. Basically, there is a competition between these two factors to modify the MSR. We keep increasing the strength of λ for fixed A, which eventually leads to the collapse of the condensate. The RIB decreases by increasing the strength of λ, LIB does not change substantially and the tunnelling of the condensate through RIB increases. As a consequence, we find that r_{av} increases slowly which leads to the decrease of $|V_{\mathrm{int}}|$ and T with a considerable growth of V_{trap}. The behaviour is very crucial as it is different from our earlier study of collapse of the attractive BEC in the harmonic trap. But we find that, the total ground-state energy (E_0) becomes low as λ increases which is analogous with our previous work for the harmonic trapping. The result is attributed to the effect of anharmonicity as it pulls down the outer part of the effective many-body potential. On the other hand, for the blue-shifted anharmonic trap ($\lambda > 0$), there is no intermediate barrier on the right side of MSR and its outer part grows more steeply at larger r as λ increases. This induces the atoms to accumulate at the minimum of the MSR and tunnelling through LIB is responsible for the system to emerge. By employing the WKB approximation, we calculate the tunnelling probabilities (P_t) of such systems. Our investigation is significant as P_t increases with the strengthening of λ. The tunnelling of the condensate through LIB into the inner core (NAW) is associated with a critical value of λ, beyond which the attractive condensate collapses. We obtain the complete quantitative description of V_{int}, V_{trap}, T and find similar change as observed in our earlier study with the attractive BEC in harmonic trap to collapse the condensate. However, in contrast with earlier finding, we have seen considerable increase of E_0 as λ increases to achieve the collapse. This dramatic behaviour is assigned by the upward shift of the MSR which is raised by the quartic term of the trapping potential.

In conclusion we state that, our study presents a clear physical picture of modification of the metastable region of the attractive condensate, confined in anharmonic trapping potential. Ground-state properties are studied in detail to explore the role of anharmonicity in external trapping potential. An experimental trap is finite and cannot be a pure harmonic oscillator. Hence, anharmonic effects are very important. So, consideration of finite number of atoms in anharmonic trap is relevant for a real experimental situation also.

Acknowledgements

The author would like to thank Dr T K Das, Retired Professor (Dept. of Physics, University of Calcutta) and Emeritus Fellow (UGC, India) for helpful support and discussion.

References

[1] M R Matthews, B P Anderson, P C Haljan, D S Hall, C E Wieman and E A Cornell, *Phys. Rev. Lett.* **83**, 2498 (1999)
[2] K W Madison, F Chevy, W Wohlleben and J Daliberd, *Phys. Rev. Lett.* **84**, 806 (2000)
[3] J R Abo-Shaeer, C Raman, J M Vogels and W Ketterle, *Science* **292**, 476 (2001)
[4] P C Haljan, I Coddington, P Engels and E A Cornell, *Phys. Rev. Lett.* **87**, 210403 (2001)
[5] P Engels, I Coddington, P C Haljan, V Schweikhard and E A Cornell, *Phys. Rev. Lett.* **90**, 170405 (2003)
[6] G M Kavoulakis and G Baym, *New J. Phys.* **5**, 51.1 (2003)
[7] T P Simula, A A Penckwitt and R J Ballagh, *Phys. Rev. Lett.* **92**, 060401 (2004)
[8] E Lundh, A Collin and K A Suominen, *Phys. Rev. Lett.* **92**, 070401 (2004)
[9] T K Ghosh, *Eur. Phys. J. D* **31**, 101 (2004)
[10] A D Jackson, G M Kavoulakis and E Lundh, *Phys. Rev. A* **69**, 053619 (2004)
[11] M Cozzini, A L Fetter, B Jackson and S Stringari, *Phys. Rev. Lett.* **94**, 100402 (2005)
[12] H Fu and E Zaremba, *Phys. Rev. A* **73**, 013614 (2006)
[13] A Collin, *Phys. Rev. A* **73**, 013611 (2006)
[14] G Q Li, L B Fu, J K Xue, X Z Chen and J Liu, *Phys. Rev. A* **74**, 055601 (2006)
[15] D A Zezyulin, G L Alfimov, V V Konotop and V M Perez-Garcia, *Phys. Rev. A* **78**, 013606 (2008)
[16] D A Zezyulin, *Phys. Rev. A* **79**, 033622 (2009)
[17] B Chakrabarti, T K Das and P K Debnath, *Phys. Rev. A* **79**, 053629 (2009)
[18] P K Debnath and B Chakrabarti, *Phys. Rev. A* **82**, 043614 (2010)
[19] S K Haldar, P K Debnath and B Chakrabarti, *Eur. Phys. J. D* **67**, 188 (2013)
[20] S K Haldar, B Chakrabarti, S Bhattacharyya and T K Das, *Eur. Phys. J. D* **68**, 262 (2014)
[21] P K Debnath, *J. Sci. Res.* **13**(**3**), 733 (2021)
[22] S K Haldar, B Chakrabarti and T K Das, *Phys. Rev. A* **82**, 043616 (2010)
[23] D M Stamper-Kurn, M R Andrews, A P Chikkatur, S Inouye, H -J Miesner, J Stenger and W Ketterle, *Phys. Rev. Lett.* **80**, 2027 (1998)
[24] V Bretin, S Stock, Y Seurin and J Dalibard, *Phys. Rev. Lett.* **92**, 050403 (2004)
[25] S Stock, V Bretin, F Chevy and J Dalibard, *Europhys. Lett.* **65**, 594 (2004)
[26] J L Roberts, N R Claussen, S L Cornish, E A Donley, E A Cornell and C E Wieman, *Phys. Rev. Lett.* **86**, 4211 (2001)
[27] J L Roberts, N R Claussen, J P Burke, J C H Greene, E A Cornell and C E Wieman, *Phys. Rev. Lett.* **81**, 5109 (1998)
[28] S L Cornish, N R Claussen, J L Roberts, E A Cornell and C E Wieman, *Phys. Rev. Lett.* **85**, 1795 (2000)
[29] A Kundu, B Chakrabarti, T K Das and S Canuto, *J. Phys. B* **40**, 2225 (2007)
[30] T K Das, S Canuto, A Kundu and B Chakrabarti, *Phys. Rev. A* **75**, 042705 (2007)
[31] T K Das and B Chakrabarti, *Phys. Rev. A* **70**, 063601 (2004)
[32] P A Ruprecht, M J Holland, K Burnett and M Edwards, *Phys. Rev. A* **51**, 4704 (1995)
[33] G Baym and C J Pethick, *Phys. Rev. Lett.* **76**, 6 (1996)
[34] F Dalfovo and S Stringari, *Phys. Rev. A* **53**, 2477 (1996)
[35] H T C Stoof, *J. Stat. Phys.* **87**, 1353 (1997)
[36] M Ueda and A J Leggett, *Phys. Rev. Lett.* **80**, 1576 (1998)

[37] B Chakrabarti, T K Das and P K Debnath, *J. Low Temp. Phys.* **157**, 527 (2009)
[38] P K Debnath, B Chakrabarti and T K Das, *Int. J. Quant. Chem.* **111**, 1333 (2011)
[39] F Dalfovo, S Giorgini, L P Pitaevskii and S Stringari, *Rev. Mod. Phys.* **71**, 463 (1999)
[40] S Geltman, *Chem. Phys. Lett.* **418**, 163 (2006)
[41] M F de la Ripelle, *Ann. Phys. (N.Y.)* **147**, 281 (1983)
[42] M F de la Ripelle, *Few-Body Syst.* **1**, 181 (1986)
[43] P K Debnath, B Chakrabarti, T K Das and S Canuto, *J. Chem. Phys.* **137**, 164106 (2012)
[44] B Chakrabarti and T K Das, *Phys. Rev. A* **78**, 063608 (2008)
[45] T K Das, A Kundu, S Canuto and B Chakrabarti, *Phys. Lett. A* **373**, 258 (2008)
[46] S A Sofianos, T K Das, B Chakrabarti, M L Lekala, R M Adam and G J Rampho, *Phys. Rev. A* **87**, 013608 (2013)
[47] J L Ballot and M F de la Ripelle, *Ann. Phys. (N.Y.)* **127**, 62 (1980)
[48] M Abramowitz and I A Stegun, *Handbook of mathematical functions* (Dover Publications, New York, 1972) p. 773
[49] C J Pethick and H Smith, *Bose–Einstein condensation in dilute gases* (Cambridge University Press, Cambridge, 2001) Vol. 1, p. 105
[50] T K Das, H T Coelho and M F de la Ripelle, *Phys. Rev. C* **26**, 2281 (1982)